Additional risk in extreme precipitation in China from 1.5 °C to 2.0 °C global warming levels

Wei Li, Zhihong Jiang, Xuebin Zhang, Laurent Li, Ying Sun

This is an accepted manuscript. The final paper can be found at https://doi.org/10.1016/j.scib.2017.12.021

Additional risk in extreme precipitation in China from 1.5°C to 2.0°C global warming levels

Wei Li
Key Laboratory of Meteorological Disaster of Ministry of Education, Collaborative Innovation Center on Forecast and Evaluation of Meteorological Disaster, Nanjing University of Information Science and Technology, Nanjing, China

Zhihong Jiang*
Joint International Research Laboratory of Climate and Environment Change, Collaborative Innovation Center on Forecast and Evaluation of Meteorological Disaster, Nanjing University of Information Science and Technology, Nanjing, China

Xuebin Zhang
Climate Research Division, Environment and Climate Change Canada, Toronto, Ontario M3H 5T4, Canada

Laurent Li
Laboratoire de Météorologie Dynamique, CNRS, Sorbonne Universités,
UPMC Université Paris 06, Paris, France

Ying Sun
National Climate Center, Laboratory for Climate Studies, China Meteorological Administration, Beijing 100812, China

* Corresponding Author: Zhihong Jiang, Key Laboratory of Meteorological Disaster of Ministry of Education, Collaborative Innovation Center on Forecast and Evaluation of Meteorological Disasters, Nanjing University of Information Science & Technology, Nanjing, 210044, China
E-mail: zhjiang@nuist.edu.cn

Abstracts

To avoid dangerous climate change impact, the Paris Agreement sets out two ambitious goals: to limit the global warming to be well below 2 °C and to pursue effort for the global warming to be below 1.5 °C above the pre-industrial level. As climate change risks may be region-dependent, changes in magnitude and probability of extreme precipitation over China are investigated under those two global warming levels based on simulations from the Coupled Model Inter-Comparison Projects Phase 5. The focus is on the added changes due to the additional half a degree warming from 1.5 °C to 2 °C. Results show that regional average changes in the magnitude do not depend on the return periods with a relative increase around 7% and 11% at the 1.5 °C and 2 °C global warming levels, respectively. The additional half a degree global warming adds an additional increase in the magnitude by nearly 4%. The regional average changes in term of occurrence probabilities show dependence on the return periods, with rarer events (longer return periods) having larger increase of risk. For the 100-year historical event, the probability is projected to increase by a factor of 1.6 and 2.4 at the 1.5 °C and 2 °C global warming levels, respectively. The projected changes in extreme precipitation are independent of the RCP scenarios.

Key words: 1.5˚C and 2˚C global warming, Extreme precipitation, China

1. Introduction

A global-scale warming has been dominating the Earth climate since the beginning of the industrial era. But to different magnitudes of temperature increase, the corresponding climate changes would exert different impacts on the global natural ecosystems and human societies. The question that what level of global warming is regarded as a dangerous warming threshold has been widely debated. The current international agreement about avoiding dangerous climate change impact was made under the United Nations Framework Convention on Climate Change (UNFCCC) at the 21st Conference of Parties (COP 21) in Paris. The agreement including two global warming targets: "holding the increase in the global average temperature to be well below 2 °C above pre-industrial and to pursue effort to limit the temperature increase to 1.5 °C." It is based on the hypothesis that maintaining the global warming below 1.5 °C would reduce the risks caused by climate change [1]. Meanwhile, UNFCCC invited the IPCC to elaborate a special report on the issue, which should be a comprehensive synthesis of the relevant scientific literature [2], [3], [4], [5], [6], [7]. The global mean warming is just an emblematic indicator, and vulnerability to global warming may vary from region to region and exhibit notable spatial inhomogeneity [3]. Therefore a differentiation of risks caused by climate change between 1.5 °C and 2 °C global warming levels is particularly important for highly sensitive regions [6]. China, a country with fragile ecological environment due to the fact that it has a prominent monsoon climate and has complex topography, is identified as a vulnerable region to global warming [8]. Floods after extreme precipitation cause considerable economic losses and serious damage to property. Therefore, it is necessary to rigorously assess physical and statistical characteristics of regional extreme precipitations when the global temperature increases by 1.5 °C and 2.0 °C relative to pre-industrial.

Global climate models are primary tools for investigating possible future change in climate extremes [9], [10], [11]. The Coupled Model Intercomparison Project Phase 5 (CMIP5) of the World Climate Research Programme incorporates more physical processes and higher resolution models than its previous phases [12]. Many results indicated that CMIP5 models can well reproduce the observed extreme precipitation at continental scale [13], [14] and regional scale [15], [16]. Climate responses to different global warming levels over China have been investigated in several recent studies using CMIP5. They mainly focus on the 2 °C warming target, including the timing of occurrence and the factors responsible for the timing uncertainties among models [17], [18]. This needs to investigate whether the expected changes exceed the natural internal variability [19], [20]. There are also researches investigating the extreme climate change with different warming targets (e.g. 2 °C, 3 °C, 4 °C) [21], [22], [23]. Recently, a few studies are reported on the climate change under 1.5 °C warming and the difference from 2 °C warming [24], [25]. However, limited attention has been paid to investigating extreme precipitation changes in term of magnitude and probability under 1.5 °C and 2 °C warming levels.

This study uses statistical method to investigate two questions: How extreme precipitation may change under 1.5 °C and 2 °C global warming levels over China and how much is the influence of the extra half degree? Such questions are critical ones and should be addressed in an appropriate way. They are not only relevant to risk assessment and adaptation measures, but also useful to rationalize future international negotiations on climate change issues.

2. Data and Methods

2.1 Data

We use the daily precipitation datasets extracted from CMIP5 models in their historical experiments (1850–2005) with natural and anthropogenic forcing, and future simulations (2006–2100) with the Representative Concentration Pathway (RCP) scenarios [26]. In this study, we make relevant diagnostics on extreme precipitations under RCP4.5 and RCP8.5 scenarios. The reason for selecting those two scenarios is that RCP8.5 is mostly close to the observed emissions pathway, whereas RCP4.5 represents a consideration of mitigation. The first realization from each model is selected in order to treat all models equally. We select 1986–2005 as the reference period for assessment of future changes under the two warming targets.

Monthly surface air temperatures in both historical experiment and RCP scenarios are used to study the timing for the global mean temperature to reach the two warming targets for each model. Given that the observed global temperature in the reference period is 0.6 °C warmer than the pre-industrial level [27], the 1.5 °C and 2 °C warming targets relative to pre-industrial imply warming of 0.9 °C and 1.4 °C relative to the reference period, respectively. We first calculate the average global temperature anomalies from 2006 to 2100 relative to the reference period by using the area-weighted scheme which takes into account the variation of grid box areas with latitude for individual models. The anomaly time series are then divided into a few 20-year time slices to find the right period when the 0.9 °C and 1.4 °C warming thresholds occur for each model separately. The CMIP5 models used in this article and their timing to reach the two warming targets under RCPs scenarios are shown in Table 1.

There is a large difference among models when 1.5 ˚C and 2 ˚C warming targets are reached. For RCP4.5, the 20-year period of 1.5˚C warming ranges from [2013, 2032] for BNU-ESM to [2046, 2065] for GFDL-ESM2G. For the 2˚C warming level, the 20-year period ranges from [2029, 2048] (HadGEM2-ES, MIROC-ESM and MIROC-EMS-CHEM) to [2064, 2083] (MRI-CGCM3). When the multi-model ensemble is examined, time reaching the two warming targets under RCP8.5 is earlier than under RCP4.5. Global warming reaches 1.5˚C under RCP4.5 and RCP8.5 at [2021, 2040] and [2016, 2035] respectively. The 2˚C warming is projected to be reached at [2041, 2060] for RCP4.5 and [2031, 2050] for RCP8.5. These results are consistent with former researches [6, 7, 18].

2.2 Methodology

Return value of annual daily precipitation is a widely used metric to measure the magnitude of extreme events [28], [29]. Also, return value is commonly used for a wide range of applications on engineering planning, for instance, in the decision of hydrologic design, water management structure, dams, and bridges. The return value for a particular return period τ is the threshold likely to be exceeded in a year with probability 1/τ. Higher τ means more intense and rarer extreme events. To estimate the return value, annual maximum (AM) approach is used to select sample sequences from daily data at every grid point to be fitted by generalized extreme value (GEV) distribution. GEV distribution has been found suitable as a fit to the tails of the distribution for precipitation. GEV distribution is also a generally reasonable approximation for the distribution of annual extremes in most CMIP5 models [14].

The cumulative distribution function, G(z), is given by (Coles, 2001) [30]:

$$\mathrm{G(z)} = \exp\left\{-\left[\xi\left(\frac{z-\mu}{\sigma}\right)\right]^{-1/\xi}\right\}, 1+\ \xi\ \left(\frac{z-\mu}{\sigma}\right) > 0$$

where μ, σ and ξ are location, scale and shape parameters, respectively. These three parameters are estimated by the method of "L-moments", which is more efficient and generates less uncertainty compared to other methods to estimate parameters over a small sample size [31]. Having estimated the parameters, return value, z_p , corresponding to the return period $\tau = 1/\mathrm{p}$, can be determined after inverting the GEV cumulative distribution function.

$$z_p = \mu - \frac{\sigma}{\xi}\left[1 - \{-\log(1-p)\}^{-\xi}\right], \xi \neq 0$$

where p is an exceedance probability. In addition, we can examine the probability change of extreme precipitation by using probability ratio (PR), a metric characterizing the factor by which probability of an event has changed [32, 33], defined as PR=P_1/P_0, where P_0 denotes the probability of τ_0-year return value during the reference period and P_1 during 1.5˚C or 2˚C warming climate, expressed as a future return period $\tau_1 = 1/P_1$, $P_1/P_0 = \tau_0/\tau_1$. If PR>1, probability of reference period events would increase at 1.5˚C or 2˚C warming environment.

Three different return periods events (20-, 50-, and 100-year) of annual maxima precipitation for the reference period (1986-2005) and the 20-year slices when global warming reaches the two warming levels for individual models are derived from the fitted GEV. PR of historical (for three return periods) events at the two levels of warming climate can also be determined. Those two statistical values from different models are interpolated onto a common 1°×1° latitude-longitude grid with a bilinear interpolation scheme.

Additionally, GEV distribution allows the incorporation of covariates in parameters to estimate the dependence of extreme precipitation change on global mean temperature anomaly, which can provide more information about extreme precipitation change with further global warming. Here, the location and scale parameters are assumed to be function of global mean temperature anomaly and the shape parameter is kept constant. Because the scale parameter must be positive everywhere, it is often modeled using a log link function, such that:

$$\mu(\mathrm{t}) = \mu_0 + \mu_1 y(t)$$

$$\ln\sigma(\mathrm{t}) = \sigma_0 + \sigma_1 y(t)$$

where y(t) is the global mean temperature anomaly from 1961 to 2100 relative to the pre-industrial in year t. $\mu_0, \mu_1, \sigma_0, \sigma_1$ are regression parameters to be estimated. The cumulative distribution function, $\mathrm{G}(z_t)$ can be expressed as

$$\mathrm{G}(z_t) = \exp\left\{-\left[\xi\left(\frac{z_t - \mu(t)}{\sigma(t)}\right)\right]^{-1/\xi}\right\}, 1 + \xi\left(\frac{z_t - \mu(t)}{\sigma(t)}\right) > 0$$

Return value Z_{p_t} is defined as

$$Z_{p_t} = \mu_t - \frac{\sigma_t}{\xi}\left[1 - \{-\log(1-p)\}^{-\xi}\right], \xi \neq 0$$

There are five parameters $(\mu_0, \mu_1, \sigma_0, \sigma_1, \zeta)$ in nonstationary GEV distribution. Those five parameters are estimated by the method of maximum likelihood estimation (MLE) [34]. An advantage of MLE is that it is efficient when the sample size is large and it is particularly preferred in estimating parameters for nonstationary data. Here, nonstationary GEV is fitted to time series of annual maxima precipitation for the period 1961-2100 for individual models. The magnitude and probability change relative to historical at given global warming target can be derived from fitted nonstationary GEV.

3. Results

3.1 Changes in the magnitude of extreme precipitation

Changes in magnitude of extreme precipitation relative to the reference period at the two warming levels under RCP4.5 and RCP8.5 were analyzed with the annual precipitation maxima from individual CMIP5 models fitted to stationary GEV (Fig. 1). Regionally averaged, the relative changes of return periods in the multi-model ensemble mean (MME) (black point) under RCP4.5 are close to RCP8.5 scenario. This indicates that changes in magnitude of extreme precipitation are not very much independent on emission scenarios when the global warming level reaches a given warming target.

t can be seen that there is little difference among return periods under same warming conditions. The amplitude is projected to increase by about 7% and nearly 11% when global warming reaches to 1.5 °C and 2 °C, respectively. Extra half a degree warming makes the intensity to increase by nearly 4%. If we use the dispersion of models to represent the projection uncertainties, we can see that the projection uncertainties vary among return periods, with larger uncertainty at higher return period. Meanwhile, uncertainties at higher warming level are larger than that at lower warming level.

We examine now the spatial distribution of intensity difference between the 1.5 °C and 2 °C worlds for RCP4.5 and RCP8.5 scenarios (Fig. 1S). As expected, the changes in 20-, 50-, and 100-year return value show a very similar spatial distribution. Compared to 1.5 °C warming, the magnitude of extreme precipitation is projected to increase under 2 °C warming across most of the region for both scenarios. In many regions where the magnitude increases, especially for regions with large increase, the consistency among models is high. Areas where large increases are projected to occur show a dependence on scenarios. Areas with an increase larger than 5% are concentrated in most of Western China and Southeastern China for RCP4.5, while for RCP8.5, such areas of increase are mainly in Western China and North China, but not in Southeastern China. These results are generally in agreement with previous studies showing that a larger magnitude of extreme precipitation can be found in those regions under the context of global warming [35], [11], [36]. The difference in intensity change between RCP4.5 and RCP8.5 also indicates that the finer change of extreme precipitation at regional scale from global models still have large uncertainties.

The magnitude change of extreme precipitation with future global warming can also be seen if the nonstationary GEV scheme is applied to the transient simulations. Fig. 2 displays the regional average changes (which is relative to reference period) of the three return periods as a function of global mean temperature anomaly (which is relative to pre-industrial) simulated by CMIP5 models for RCP4.5 and RCP8.5 scenarios. It is noted that the global warming in the multi model ensemble mean do not exceed 3 °C relative to pre-industrial for RCP4.5 and 5 °C for RCP8.5 scenario, so we only show the relationship within the period where global warming may reach. Results of non-stationary calculation show very similar results as in the stationary calculation. This is particularly true for the change of magnitude in MME and uncertainties among models when warming reaches 1.5 °C and 2 °C. The nonstationary results show that the magnitude increases in MME nonlinearly with future warming. For example, the magnitude is expected to increase by nearly 8% when global mean temperature warms from 1 °C to 2 °C, while the increase is about 5% when the global mean temperature increases from 3 °C to 4 °C under RCP8.5.

3.2 Change in the probability of extreme precipitation

The probability change of historical extreme events at two warming levels is analyzed in this section. The regional average PR of historical events for the three return periods is illustrated in Fig. 3 for the two warming levels. As expected, the MME results show little distinction between RCP4.5 and RCP8.5 scenarios. Generally speaking, the probabilities of historical extreme events are projected to increase in response to the global warming. PR increases most strongly for the longest return periods, especially at higher warming level, which implies that the most intense and rarest extreme precipitation events have largest increase in the risk. Taken 2 °C warming as an example, the probability of historical 20-yr events increases by a factor of 1.9, however, for historical 100-year events, the probability increases by a factor of 2.4.

Probability of historical 100-year events increases by about a factor of 1.6 under 1.5 °C warming and 2.4 under 2 °C warming climate. This implies that regional average event expected once every 100 years in historical period is expected to occur about every 62 and 42 years under 1.5 °C and 2 °C warming climate, respectively. The 100-year event of 1.5 °C warming is almost 1.4 times more likely to occur at 2 °C warming.

Similar to the relative changes of magnitude in extreme precipitation, the inter-model variation of PR is significant across the three return periods for a given warming level, with larger inter-model spreading at higher return periods. For example, PR of a historical 20-year event ranges from 1.4 to 2.8 under 2 °C warming level, but for 100-year events, PR ranges from 1.6 to 4.2. Furthermore, the inter-model spreading of PR under higher warming climate is also larger. PR of a historical 100-year event at 1.5 °C and 2 °C warming levels ranges from 1.0 to 2.6 and 1.6 to 4.2, respectively.

The spatial distribution of PR variation between 1.5 °C warming and 2 °C warming is also researched (Fig. 2S). We show the cases for 20-, 50-, and 100-year events and for the two scenarios. The risk of extreme events at 1.5 °C warming level is projected to increase almost everywhere at 2 °C warming over China for both RCP scenarios. PR of 20-, 50-, and 100-year events shows a very similar spatial distribution, although it varies depending on the return periods with higher return periods associated to larger PR. Areas where PR is larger than 2.0 show a future strengthening and extension with increasing of return periods. Those regions also depend on scenarios. The largest PR for RCP4.5 is projected to occur over large zones in western China, especially around the Tibetan Plateau. For RCP8.5, the largest PR occurs over western China and the Yangtze River. Events that would be attained once every 50 and 100 years in 1.5 °C warming climate will be 2 times more likely to occur at 2 °C warming climate in those regions. Meanwhile, regions with large increase of probability also exhibit a relative high models consistency.

In order to study how the probability changes with future global warming, we examine the probability change of historical extreme events with increases of global mean temperature by using the non-stationary GEV distribution. Fig. 4 displays the regional average PR of historical extreme events at a given warming levels relative to pre-industrial conditions in CMIP5 models for RCP4.5 and RCP8.5 scenarios. Also, results of PR exhibit no difference between the stationary and nonstationary schemes for MME and inter-model spread. However, with further warming, the PR of historical events in MME increases nonlinearly, especially for the very rare events. The probability of historical 100-year events increases 2 times when global warming increases from 4 °C to 5 °C. However, when global warming increases from 1 °C to 2 °C, the probability of historical 100-year events only increases 1 time. It is also noted that the uncertainties among models would be larger at higher warming. For instance, the range of models for PR of 100-year historical events at 4 °C warming is nearly 13 times higher than that at 1 °C warming.

4. Summary

In this study, future changes in magnitude and probability of extreme precipitation are investigated at global warming levels of 1.5˚C and 2˚C above pre-industrial. The magnitude and probability of extreme precipitation are described by the return values corresponding to three return periods and probability risk, respectively. Major findings are summarized as follows.

(1) Changes of extreme precipitation from MME show less dependences on the emission scenarios of RCP4.5 and RCP8.5 when global warming reaches two warming levels.

(2) Relative changes in the magnitude exhibit little difference for different return periods under the same warming threshold. Magnitude is projected to increase by

about 7% for 1.5˚C warming and 11% for 2˚C warming relative to reference period. The additional half a degree warming makes the extreme precipitation to increase by 4%.

(3) Probabilities of a given change depend on the return periods. The rarest events (the longest return period) have largest increase in the risk for a given warming level. For historical 100-year events, their occurrence probability increases by 1.6 times at 1.5˚C warming, whereas at a 2˚C warming, the increase is about 2.4 times. The 100-year event of 1.5˚C is 1.4 times more likely to occur at 2˚C warming condition.

(4) Uncertainties among models for magnitude and probability of change increase with global warming and higher return period events exhibits larger uncertainties.

Our research is one of the first studies targeting two global warming levels at 1.5˚C and 2˚C over China. For both of them, extreme precipitation shows stronger magnitude and higher probability. Changes are generally larger under 2˚C global warming level compared to 1.5˚C global warming. The additional half-degree warming does matter for eventual mitigation measures against extreme precipitation events. We should remind that global climate models are generally of low spatial resolution and they suffer imperfections for physical processes, which causes differences and uncertainties among models in projecting regional-scale climate changes. Some regional climate modelling efforts in East Asia show that a higher resolution may give a more accurate regional climate [37-39]. Therefore, more experiments with higher-resolution regional climate models are needed to address this issue of regional climate change.

Acknowledgments

We acknowledge the World Climate Research Programme's Working Group on Couple modelling and the modeling groups listed in Table S1 of this paper for making their simulations available for analysis, the PCMDI for collecting and archiving the CMIP5 model output (http://pcmdi9.llnl.gov.) This work is supported by the National Key R&D Program of China (Grant 2017YFA0603804), the State Key Program of

National Natural Science Foundation of China (41230528), and the China Scholarship Council (CSC) under the State Scholarship Fund. L. Li was partly supported by the French ANR Project China-Trend-Stream.

Reference

1. UNFCCC: Decision 1/CP.21, The Paris Agreement. 2015.
2. Donnelly C, Greuell W, Andersson J, et al. Impacts of climate change on European hydrology at 1.5, 2 and 3 degrees mean global warming above preindustrial level. Clim Change, 2017; 143: 1-14.
3. Schleussner, C, Lissner, T, Fischer E, et al. Differential climate impacts for policy-relevant limits to global warming: the case of 1.5˚C and 2˚C, Earth Syst Dyn, 2016; 7: 327–351.
4. King A D, Karoly, D J, Henley, B J. Australian climate extremes at 1.5˚C and 2˚C of global warming. Nat Clim Change, 2017; 7(6): 412-416.
5. Schaeffer M, Hare W, Rahmstorf S, Vermeer M. Long-term sea-level rise implied by 1.5˚C and 2˚C warming levels. Nat Clim Change, 2012; 2(12):867.
6. Seneviratne S I, Donat M G, Pitman A J, et al. Allowable CO2 emissions based on regional and impact-related climate targets, Nature, 2016; 1870, 1-7.
7. Karmalkar A V, Bradley R S. Consequences of Global Warming of 1.5˚C and 2˚C for Regional Temperature and Precipitation Changes in the Contiguous United States. PloS one, 2017; 12(1): e0168697.
8. Huang, J., Liu, Y., Ma, L., and Su, F. Methodology for the assessment and classification of regional vulnerability to natural hazards in China: the application of a DEA model. *Natural hazards*, 2013; *65*(1), 115-134.
9. Sillmann, J., Kharin, V. V., Zwiers, F. W., Zhang, X., and D. Bronaugh. Climate extremes indices in the CMIP5 multimodel ensemble: Part 2. Future climate projections, *J. Geophys. Res.-Atmos., 2013,* 118(6), 2473-2493.
10. Knutti, R., and J. Sedláček .Robustness and uncertainties in the new CMIP5 climate model projections, *Nature Climate Change,2013;* 3(4), 369-373.
11. Li, W., Jiang, Z., Xu, J., and L. Li, Extreme Precipitation Indices over China in CMIP5 Models. Part II: Probabilistic Projection, *J. Climate,2016;* 29(24), 8989-9004.
12. Taylor, K. E., Stouffer, R. J., & Meehl, G. A. (2012). An overview of CMIP5 and the experiment design. Bulletin of the American Meteorological Society, 93(4), 485-498.
13. Sillmann, J., Kharin, V. V., Zhang, X., Zwiers, F. W., and Bronaugh, D. Climate extremes indices in the CMIP5 multimodel ensemble: Part 1. Model evaluation in the present climate. *Journal of Geophysical Research: Atmospheres*, 2013; *118*(4), 1716-1733.
14. Kharin, V. V., Zwiers, F. W., Zhang, X., and Wehner, M. Changes in temperature and precipitation extremes in the CMIP5 ensemble. *Climatic change*, 2013; *119*(2), 345-357.
15. Jiang, Z., Li, W., Xu, J., and Li, L. Extreme precipitation indices over China in CMIP5 models. Part I: Model evaluation. *Journal of Climate*, 2015; *28*(21), 8603-8619.

16. Ou, T., D. Chen, H. W. Linderholm, and J. H. Jeong. Evaluation of global climate models in simulating extreme precipitation in China. Tellus, 2013; 65A, 1393–1399,
17. Chen X, and Zhou T. Uncertainty in crossing time of 2˚C warming threshold over China. Chin Sci Bull, 2016; 61(18): 1451-1459.
18. Zhang L, Ding Y, Wu T, Xin X, Zhang Y, Xu Y. The 21st century annual mean surface air temperature change and the 2°C warming threshold over the globe and China as projected by the CMIP5 models. Acta Meteorol Sin, 2013; 71(6): 1047-1060
19. Jiang D B, Yue S, and Lang X. Timing and associated climate change of a 2°C global warming. Int J Climatol, 2016; 36(14): 4512-4522.
20. Sui Y, Lang X, Jiang D. Temperature and precipitation signals over China with a 2°C global warming. Clim Res, 2015; 64(3):227-242.
21. Jiang D B, Zhang Y, and Sun J. Ensemble projection of 1–3°C warming in China. Chin Sci Bull, 2009; 54(18): 3326-3334.
22. Guo X, Huang J, Luo Y, et al. Projection of precipitation extremes for eight global warming targets by 17 CMIP5 models. Nat Hazards, 2016; 84(3): 2299-2319.
23. Tian, D., W. Dong, H. Zhang, et al. Future changes in coverage of 1.5 °C and 2 °C warming thresholds. Sci Bull, 62 (2017), pp. 1455-1463
24. Chen J, Gao C, Zeng X, et al. Assessing changes of river discharge under global warming of 1.5° C and 2° C in the upper reaches of the Yangtze River Basin: Approach by using multiple-GCMs and hydrological models. Quat Int, 2017; 435: 63-73.
25. HU, T., SUN, Y., & ZHANG, X. (2017). Temperature and precipitation projection at 1.5 and 2° C increase in global mean temperature. *Chinese Science Bulletin*, *62*(26), 3098-3111.
26. Moss, R. H., Edmonds, J. A., Hibbard, K. A., et al. The next generation of scenarios for climate change research and assessment. Nature, 2010; 463(7282), 747-756.
27. Harmann D L, Klevin Tank A M G, Rusticucci M, et al. Observations: Atmosphere and Surface. In: Stocker T F, Qin D H, Plattner G K, et al., eds. Climate Change 2013: The Physical Science Basis. Contribution of Working Group I to the Fifth Assessment Report of the Intergovernmental Panel on Climate Change. Cambridge: Cambridge University Press, 2013; 159-254
28. Zhang Y, Gao Z, Pan Z. Li D, et al. Spatiotemporal variability of extreme temperature frequency and amplitude in China. Atmos Res, 2017; 185: 131-141.
29. Kharin V V, Zwiers F W, Zhang X, et al. Changes in temperature and precipitation extremes in the IPCC ensemble of global coupled model simulations. J Climate, 2007; 20(8): 1419-1444.
30. Coles S. An Introduction to Statistical Modeling of Extreme Values, Springer-Verlag, 2001; 208 pp.
31. Hosking J M R and James R W. Regional frequency analysis: an approach based on L-moments. Cambridge University Press, 2005.
32. Stott P A, Dáithí A S, and Myles R A. Human contribution to the European heatwave of 2003. Nature, 2004; 432(7017): 610-614.
33. Fischer E M and Knutti R. Anthropogenic contribution to global occurrence of heavy-precipitation and high-temperature extremes. Nat Clim Change, 2015; 5(6):

560-564.
34. Martins E S and Stedinger J R. Generalized Maximum Likelihood Pareto-Poisson estimators for partial duration series. Water Resour Res, 2001; 37(10): 2551-2557.
35. Chen H P. Projected change in extreme rainfall events in China by the end of the 21st century using CMIP5 models. Chin Sci Bull, 2013; 58: 1462–1472
36. Wang L, Chen W. A CMIP5 multimodel projection of future temperature, precipitation, and climatological drought in China. Int J Climatol, 2014; 34(6): 2059-2078.
37. Yang H, Jiang Z, and Li, L. Biases and improvements in three dynamical downscaling climate simulations over China, Clim Dyn, 2016; 47(9-10): 3235-3251
38. Zou L, and Zhou, T. Future summer precipitation changes over CORDEX-East Asia domain downscaled by a regional ocean-atmosphere coupled model: A comparison to the stand-alone RCM, J Geophys Res Atmos, 2016; 121(6): 2691-2704.
39. Gao X J, Shi Y, Giorgi F. Comparison of convective parameterizations in RegCM4 experiments with CLM as the land surface model over China. Atmospheric and Oceanic Science Letters, 2016; 9(4), 246–254.

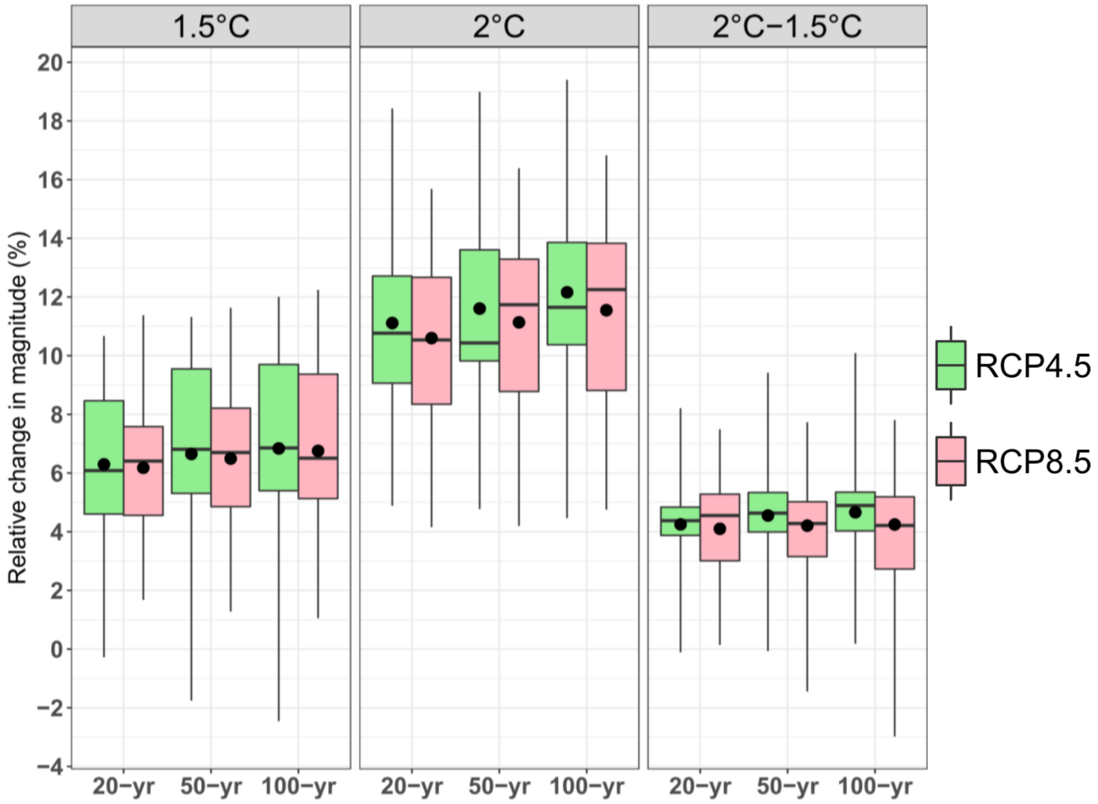

Fig.1 Boxplots of the regional average relative change (relative to 1986-2005 reference period, units: %) in the 20-, 50-, 100-year return values for 1.5˚C (left panel) and 2˚C (middle panel) warming level, as well as the difference between the two warming levels (right panel) among models under RCP4.5 and RCP8.5 scenario. The upper and lower limits of the box indicate the 75th and 25th percentile value among models; the horizontal line in the box indicates the multi-model ensemble median and the whiskers show the range of models. MME is represented by black points.

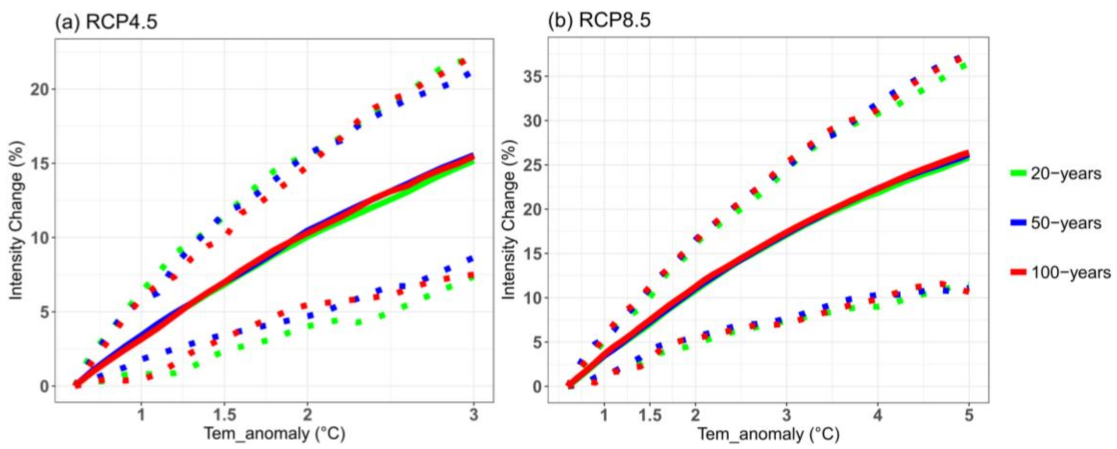

Fig.2 The relationship between relative change (%) in regional average 20- (green), 50- (blue), and 100-year (red) return values (relative to reference period) and global mean temperature anomaly (relative to pre-industrial) in CMIP5 models for RCP4.5 (a) and RCP8.5 (b). Solid lines indicate the MME and the dotted lines are the uncertainties range.

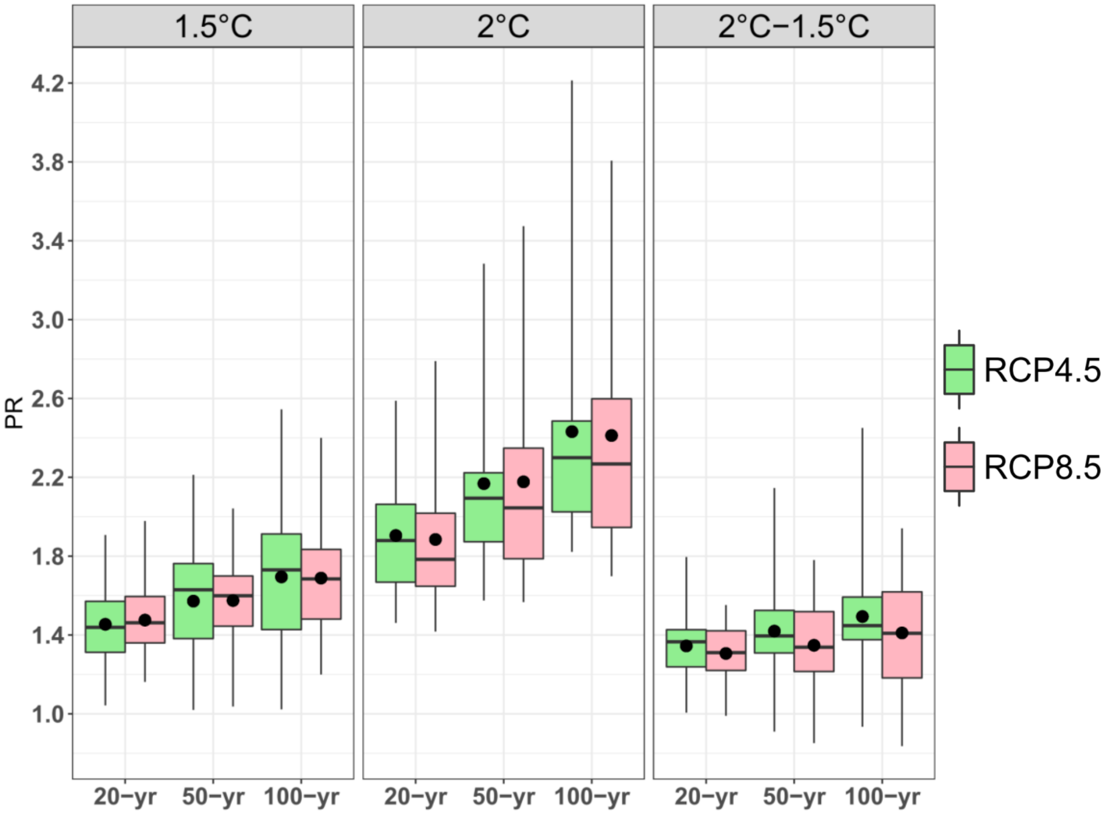

Fig.3 Boxplots of PR for the historical 20-, 50-, 100-year return values in 1.5˚C (left panel) and 2˚C (middle panel) warming conditions among models, as well as PR of 1.5˚C warming events in 2˚C warming conditions (right panel) under RCP4.5 and RCP8.5 scenarios. The upper and lower limits of the box indicate the 75th and 25th percentile value among models; the horizontal line in the box indicates the multi-model ensemble median and the whiskers show the range of models. MME is represented by black points.

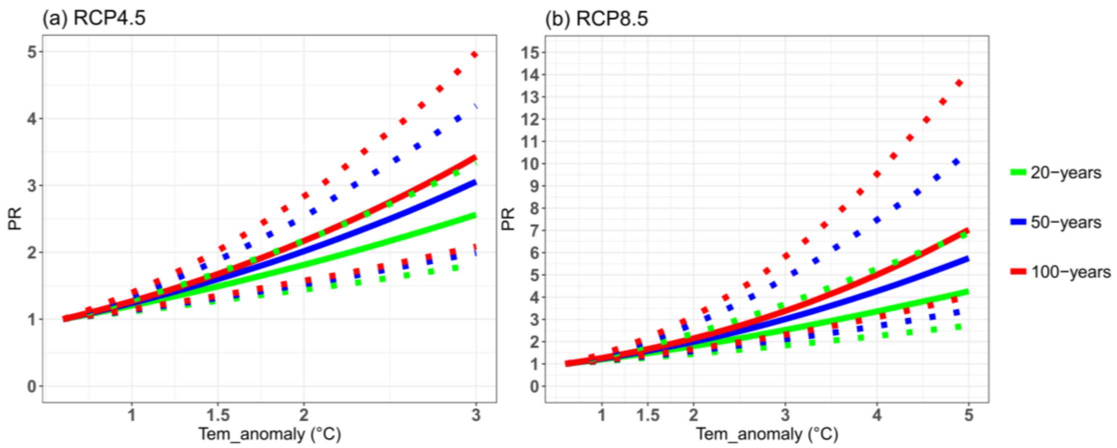

Fig. 4 The relationship between PR of historical 20- (green), 50- (blue), and 100-year (red) return values and global mean temperature anomaly (relative to pre-industrial) for RCP4.5 and RCP8.5. Solid lines indicate the MME and the two dotted lines represent the uncertainties range.

Table 1 The CMIP5 models used in this article, together with their atmospheric model's resolution and the 20-year time slices when global warming reaches 1.5˚C and 2˚C relative to pre-industrial period under RCP4.5 and RCP8.5 scenarios.

Model name	Atmospheric resolution	**RCP4.5**		**RCP8.5**	
		1.5˚C	2 ˚C	1.5˚C	2 ˚C
ACCESS1.0	~1.9°×1.25°, L38	[2018,2037]	[2041,2060]	[2016,2035]	[2029,2048]
ACCESS1.3	~1.9°×1.25°, L38	[2020,2039]	[2039,2058]	[2015,2034]	[2029,2048]
BCC-CSM1.1	~2.8°×~2.8°, L26	[2026,2045]	[2062,2081]	[2022,2041]	[2036,2055]
BCC-CSM1.1(m)	~1.1°×~1.1°, L26	[2020,2039]	[2063,2082]	[2015,2034]	[2034,2053]
BNU-ESM	~2.8°×~2.8°, L26	[2013,2032]	[2032,2051]	[2012,2031]	[2024,2043]
CanESM2	~2.8°×~2.8°, L35	[2014,2033]	[2028,2047]	[2009,2028]	[2022,2041]
CCSM4	1.25°×~0.9°, L26	[2025,2044]	[2052,2071]	[2015,2034]	[2032,2051]
CMCC-CM	0.75°×~0.75°, L31	[2024,2043]	[2041,2060]	[2028,2047]	[2040,2059]
CMCC-CMS	~1.9°×~1.9°, L95	[2022,2041]	[2039,2058]	[2017,2036]	[2029,2048]
CNRM-CM5	~1.4°×~1.4°, L31	[2029,2048]	[2051,2070]	[2022,2041]	[2036,2055]
HadGEM2-CC	~1.9°×1.25°, L40	[2017,2036]	[2033,2052]	[2008,2027]	[2022,2041]
IPSL-CM5A-LR	3.75°×~1.9°, L39	[2019,2038]	[2035,2054]	[2015,2034]	[2027,2046]
IPSL-CM5A-MR	2.5°×~1.25°, L39	[2015,2034]	[2036,2055]	[2014,2033]	[2027,2046]
MIROC5	~1.4°×~1.4°, L40	[2025,2044]	[2053,2072]	[2021,2040]	[2037,2056]
MIROC-ESM	~2.8°×~2.8°, L80	[2015,2034]	[2029,2048]	[2013,2032]	[2023,2042]
MIROC-ESM-CHEM	~2.8°×~2.8°, L80	[2014,2033]	[2029,2048]	[2010,2029]	[2022,2041]
MPI-ESM-LR	~1.9°×~1.9°, L47	[2024,2043]	[2055,2074]	[2019,2038]	[2034,2053]
MPI-ESM-MR	~1.9°×~1.9°, L95	[2027,2046]	[2048,2067]	[2022,2041]	[2036,2055]
MRI-CGCM3	~1.1°×~1.1°, L48	[2034,2053]	[2064,2083]	[2026,2045]	[2039,2058]
NorESM1-M	2.5°×~1.9°, L26	[2028,2047]	[2060,2079]	[2022,2041]	[2038,2057]